Epitaxial Growth and Processing of Compound Semiconductors

Academic and Research Staff
Professor Leslie A. Kolodziejski, Dr. Gale S. Petrich

Graduate Students
Solomon Assefa, Reginald E. Bryant, Alexei A. Erchak, Aleksandra Markina, Sheila Tandon, and Ryan Williams

Technical and Support Staff
Diane W. Hagopian and Donna L. Gale

Introduction

The emphasis of this research program is the epitaxial growth and processing of III-V compound semiconductors. The epitaxial growth of the heterostructures is performed in the chemical beam epitaxy laboratory. The laboratory consists of two gaseous source epitaxy reactors interconnected to several smaller chambers, which are used for sample introduction and in-situ surface analysis.

In the following sections, the status of the various III-V-based projects will be discussed. The III-V gas source molecular beam epitaxy system is utilized for the development of GaAs-based and InP-based bipolar cascade lasers, and for the fabrication of GaAs-based devices implementing one- and two-dimensional photonic bandgap crystals within their structure. The development of bipolar cascade lasers represents a collaboration between the research groups under the direction of Prof. Rajeev Ram and Prof. Leslie Kolodziejski. The research projects utilizing photonic crystals represent the combined efforts of the research groups led by Professors John D. Joannopoulos (Theory), Leslie A. Kolodziejski (Fabrication), Erich P. Ippen (Measurement), and Henry I. Smith (Fabrication). The complexity of the design, fabrication and characterization of these photonic crystal-based structures necessitates a strong interaction between the various research groups.

1. Development of Bipolar Cascade Laser with an Emission Wavelength of 0.98 µm

Sponsors
DARPA: #F30802-00-C-0128
DARPA/Brown University: #1123-24596

Project Staff
Ryan Williams, Aleksandra Markina, Dr. Gale S. Petrich, Professor Rajeev Ram and Professor Leslie A. Kolodziejski

Bipolar cascade lasers (BCLs) differ from typical semiconductor laser diodes by its ability to potentially produce more than one photon for every carrier injected into the device. This ability to achieve a quantum efficiency greater than 100% is accomplished by electrically and optically connecting more than one active region in series. Within MIT, gas source molecular beam epitaxy technology is used to deposit the epilayers necessary to create a BCL on GaAs substrates. These lasers contain two active regions that are connected in series by a tunnel junction, in which each active region contains an 8 nm thick $In_{0.2}Ga_{0.8}As$ quantum well with GaAs barriers. The tunnel junction consists of a highly doped p-n junction placed in reverse bias with respect to the overall laser structure. The BCL operates by first injecting a carrier into the first quantum well, where it experiences a radiative interband transition. The carrier then tunnels from the first active region to the second active region, where it undergoes another radiative interband transition. Hence, a single injected carrier experiences multiple radiative transitions, thereby achieving greater than 100% quantum efficiency.

The tunneling event in the laser is critical to its operation. The probability of tunneling is proportional to the bandgap of the semiconductor material used in the junction. A cascade laser has already been demonstrated using a GaAs tunnel junction [1,2]. The incorporation of indium into the tunnel junction will

lower the bandgap of the material and should increase the tunneling probability, as the carriers now face a smaller tunneling energy barrier. Several tunnel junctions with different indium compositions are being studied to better understand this relationship.

Optical communication requirements make it highly desirable to have single mode lasers. A novel laser structure is being studied which combines the cascade laser design with an antiresonant cavity to produce single mode emission. The antiresonant reflecting optical waveguide bipolar cascade laser (ARROW-BCL) has been studied theoretically and is moving towards the realization of an actual device structure. An ARROW-BCL laser could be used to effectively couple to an optical fiber while producing net optical gain, making the structure desirable for communications applications.

References

1. S. G. Patterson, G. S. Petrich, R. J. Ram, and L. A. Kolodziejski, "Continuous-wave room temperature operation of bipolar cascade laser", Electronic Letters, 35(5): 395-397, (1999)
2. S. G. Patterson, *Bipolar Cascade Lasers*, Ph.D. Thesis, Department of Electrical Engineering and Computer Science, MIT, (2000)

2. Development of Bipolar Cascade Laser with an Emission Wavelength of 1.57μm

Sponsors
DARPA: #F30802-00-C-0128

Project Staff
Aleksandra Markina, Ryan Williams, Dr. Gale S. Petrich, Professor Rajeev Ram and Professor Leslie A. Kolodziejski,

Bipolar Cascade Laser (BCL) consists of several single stage lasers coupled by tunnel junctions. BCLs can achieve high quantum efficiencies (the ratio of the number of emitted photons to the number of injected electrons) because an injected electron can participate in more than one recombination event by tunneling from one laser stage to the next. The first room temperature, continuous wave operation of a two-stage BCL at 990 nm was recently achieved [1,2]. This project aims to develop, fabricate, and characterize an InGaAsP/InP BCL structure with an emission wavelength λ=1.57 μm, catering to a λ=1.55 μm lightwave communication system.

The two main elements of the project are the development of a single stage semiconductor laser and the building of a tunnel junction. The chosen material system, (InGa)(AsP), offers a range of bandgap energies compatible with all-optical fiber networks and can be grown by gas source molecular beam epitaxy (GSMBE) on InP substrates. GSMBE growth is effectively used to achieve atomically abrupt doping and refractive index profiles.

A single stage laser structure has been designed and grown by GSMBE. The band structure is designed to confine carriers in the active region, which is much shorter than the carriers' diffusion length. In addition, the active layer is designed to have a larger index of refraction than the cladding layers, leading to the confinement of light to the active region. Thus, the active region essentially represents an optical waveguide. In the current design, dopant-graded InP layers surround an active $In_{0.56}Ga_{0.44}As_{0.93}P_{0.07}$ layer and $In_{0.91}Ga_{0.09}As_{0.2}P_{0.8}$ cladding layers. In order to make the device polarization insensitive, the quaternary layers are closely lattice matched to InP [3]. The active layer has a bandgap that corresponds to a wavelength of 1.57 μm.

A tunnel junction is a crucial element of a BCL. In a BCL, a tunnel junction is operated in reverse bias, allowing electrons to tunnel from the p-doped side of the junction to the n-doped side, and hence cascading between the single stage lasers. Desirable properties of tunnel junction material include narrow bandgap, high doping, and abrupt doping profile. Current work focuses on design, growth, and characterization of a series of tunnel junctions. Tunnel junction materials under investigation include Si-

and Be-doped InP and $In_{1-x}Ga_xAs_yP_{1-y}$ epilayers with bandgaps corresponding to wavelengths from 0.92 μm to 1.2 μm.

References

1. S. G. Patterson, G. S. Petrich, R. J. Ram, and L. A. Kolodziejski, "Continuous-wave room temperature operation of bipolar cascade laser", Electronic Letters, 35(5): 395-397, (1999)
2. S. G. Patterson, *Bipolar Cascade Lasers*, Ph.D. Thesis, Department of Electrical Engineering and Computer Science, MIT, (2000)
3. *Quantum Well Lasers*, ed. P.S. Zory, Jr., (Academic Press, Inc., 1993)

3. Enhanced Performance of Optical Sources in III-V Materials Using Photonic Crystals

Sponsors
National Science Foundation #DMR-9808941
Lincoln Laboratory #BX-7271

Project Staff

Alexei A. Erchak, Daniel J Ripin, Peter Rakich, Mark Mondol, Dr. Shanhui Fan, Dr. Gale Petrich, Professor Erich P. Ippen, Professor John D. Joannopoulos, Professor Henry I. Smith and Professor Leslie A. Kolodziejski

Enhanced Extraction from a Light-Emitting Diode Modified by a Photonic Crystal and Lasing Action

Semiconductor LEDs have the potential to be low-cost and long lifetime solid-state lighting sources for applications as varied as room lighting and flat-panel displays. LEDs are also used in short-range telecommunication systems and may be desirable for optical interconnects in computers. Unfortunately, most of the light emitted from a semiconductor LED is lost due to total internal reflection resulting in low extraction efficiency.

In this work, the effect of a two-dimensional (2D) photonic crystal (PC) on the emission properties of a quantum well (QW) inside a LED is examined. Enhanced extraction of light into the vertical direction is obtained and attributed to the presence of leaky resonant states created by the coherent scattering from the periodicity of the PC. The 2D PC is fabricated in the top cladding layer of an asymmetric active region that emits at λ = 980 nm with a full-width at half-maximum of approximately 60 nm at room temperature. The photoluminescence (PL) emission at 935 nm, normal to the surface, is enhanced by a factor of 100 and the spectrally integrated PL is enhanced by a factor of 8, both when compared to a reference structure without a PC. When optically pumped above threshold, lasing occurs at a wavelength of 1005 nm. This work provides a basis for the design of high efficiency LEDs and lasers based on 2D PCs.

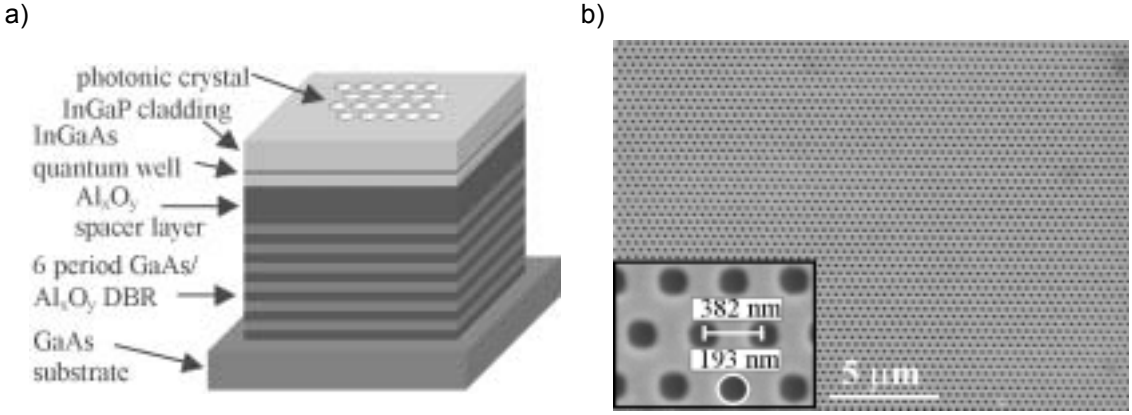

Figure 1. a) A schematic of the 2D PC structure. b) SEM micrographs of PC structure.

The 2D PC is a 30 x 30 μm triangular lattice of holes etched within the upper InGaP cladding layer of a mesa shown schematically in Figure 1(a). To minimize carrier recombination at the etched surfaces, the holes do not penetrate the InGaAs QW; however, the hole depth is sufficient to cause enhanced extraction of light and laser feedback. The device structure is grown using gas-source molecular beam epitaxy. The separation layer is initially grown as $Al_{0.98}Ga_{0.02}As$ and the distributed bragg reflector (DBR) consists of AlAs and GaAs layers. A SiO_2 layer is deposited on the grown structure using plasma-enhanced chemical vapor deposition. The holes are defined in polymethyl methacrylate (PMMA) by direct-write electron-beam lithography. The electron beam writes a square pattern in the PMMA to represent each hole. The beam size, however, is larger than the step size used to translate the electron beam which leads to the desired circular pattern following development.

The PMMA is used as a mask in transferring the triangular pattern into the SiO_2 layer using reactive ion etching (RIE). This is accomplished by RIE with a CHF_3 plasma using 15 second etches in between one minute cool-down steps. The purpose of the cool-down step is to prevent the flowing of the PMMA mask. The SiO_2 mask is subsequently used in the RIE of the holes into the upper InGaP cladding layer using a $CH_4/H_2/O_2$ plasma in a 8:8:1 gas flow ratio. The mesas are next defined using photolithography followed by RIE with the $CH_4/H_2/O_2$ plasma to etch the active region and a BCl_3 plasma to expose the mesa sidewalls. The final step in the device fabrication is the wet thermal oxidation of the $Al_{0.98}Ga_{0.02}As$ separation layer and the AlAs DBR layers. Figure 1(b) shows a PC structure with lattice constant of 382 nm, hole diameter of 193 nm, hole depth of 101 nm, and an active region thickness of 198 nm that was imaged using a scanning electron microscope (SEM); this structure is characterized and the results are reported below.

The photoluminescence (PL) is observed using a cw Ti:Al_2O_3 laser with an emission wavelength of 785 nm. Figure 2(a) shows a spectrum of the enhancement of PL from the PC region normalized to the same structure but without a PC. Figure 2(b) is a calculation of the photonic band structure near the Γ point in the first brillouin zone. The bands represent leaky resonant states that provide a pathway for the enhancement of light extraction. On the long wavelength end of the spectrum, the range covered by the first three bands closely matches the large observed peak centered near 935 nm. The width of the peak is determined by the quality factor of the leaky resonance and by the collection angle (dotted line). Band 4 and bands 5 and 6 closely match the peaks near 890 nm and 860 nm, respectively. The dip between peaks 2 and 3 corresponds well with the gap in available states between bands 3 and 4.

a) b)

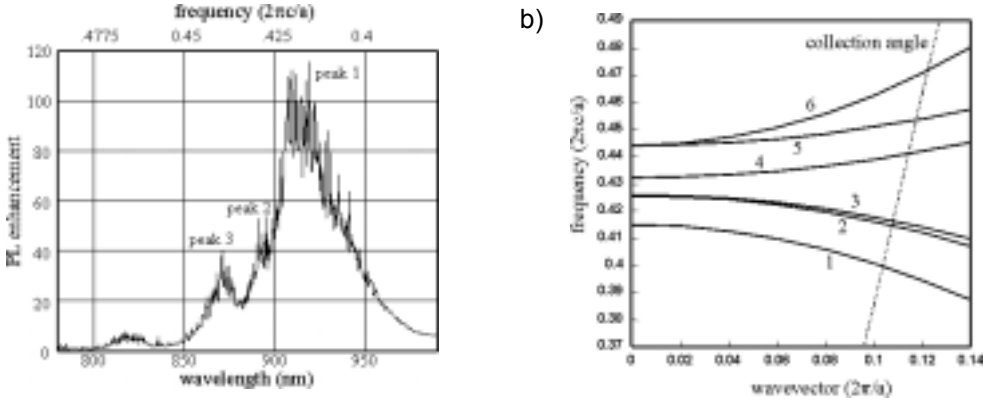

Figure 2. a) Photoluminescence enhancement spectrum from PC structure. b) Calculated photonic band structure near Γ point.

Scattering along the high-symmetry directions within the photonic crystal also provides sufficient distributed feedback for lasing to occur. Figure 3(a) shows the emission spectra from a photonic crystal optically pumped just above threshold. The lasing peak, which occurs at a wavelength of 1005 nm, corresponds with the bending of bands at the M point [Figure 3(b)].

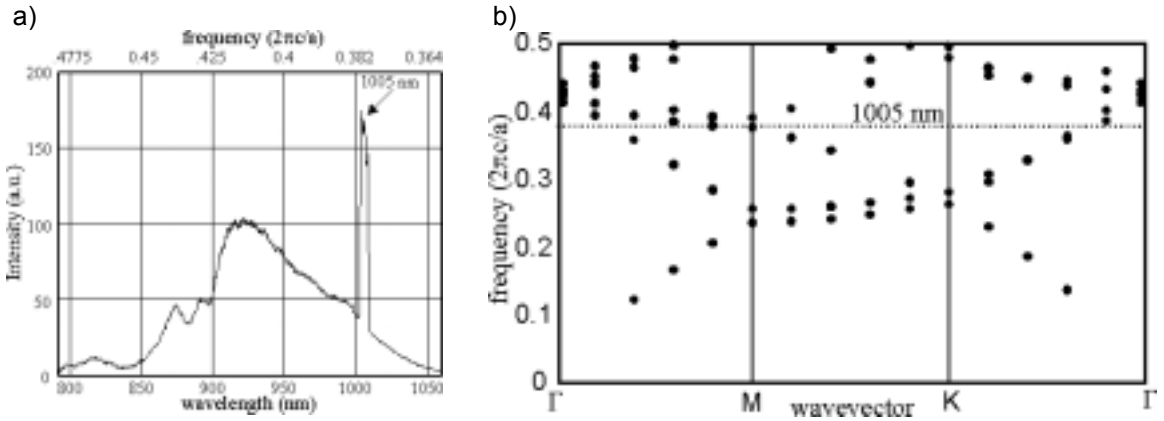

Figure 3. a) Lasing spectrum. b) Calculated band structure showing band folding near M point.

Photonic Band Gap Microcavity Laser Embedded in a Strip Waveguide

A one-dimensional (1-D) photonic crystal is fabricated within a strip waveguide to provide strong optical confinement with a small modal volume on the order of a half-cubic wavelength. The microcavity is formed by a defect in the one-dimensional periodic photonic crystal. Optical confinement is achieved in the lateral and vertical directions by high refractive index contrast. A high-efficiency, low-threshold, microcavity laser results with the light output coupling to the strip waveguide. The structure is designed to be integratable with other optoelectronic devices.

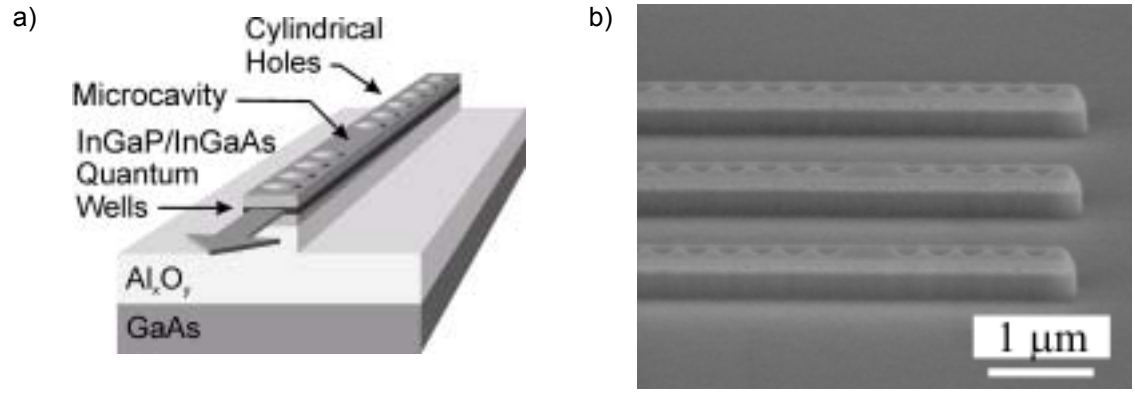

Figure 4. a) Schematic of 1-D PBG microcavity laser structure. The line of cylindrical holes forming the photonic crystal provides strong optical confinement along the waveguide. b) A SEM micrograph showing several completed microlaser structures.

The 1-D photonic band gap microcavity laser consists of an InGaP/InGaAs multiple quantum well active region emitting at λ=980 nm, on top of a low refractive index Al_xO_y spacer layer. Figure 4(a) shows a schematic of the structure. The 1-D photonic crystal consists of a periodic line of holes etched within the active region with a hole-to-hole spacing of 256 nm and a hole diameter of 113 nm. The strip waveguide width and depth are 320 nm and 112 nm, respectively. The length of the defect region is 426 nm. The active quantum well region lies on top of a low index spacer layer to separate the waveguide mode from the high index substrate. The laser output will occur on the side of the defect with the least number of holes.

The device structure is grown using gas-source molecular beam epitaxy. The separation layer is initially grown as $Al_{0.9}Ga_{0.1}As$ and graded up to higher Ga composition by dropping the Al cell temperature by

20ºC and by raising the Ga cell temperature by 20ºC in 2 minutes. The composition is graded to stabilize the interface with the active region upon oxidation of the separation layer. A SiO_2 layer is deposited on the grown structure using plasma-enhanced chemical vapor deposition. The holes and strip waveguide are defined in PMMA by direct-write electron-beam lithography. The pattern is then reversed using a Ni liftoff process. The pattern is transferred from the Ni to the SiO_2 by RIE with a CHF_3 plasma. The Ni mask is then removed using a wet Ni etchant. The SiO_2 mask is used to transfer the microlaser pattern into the InGaP/InGaAs active region using RIE with a $CH_4/H_2/O_2$ plasma with a 8:8:1 gas flow ratio. The $CH_4/H_2/O_2$ plasma etching slows at the $Al_{0.9}Ga_{0.1}As$ separation layer. Further RIE of the spacer layer is accomplished using a BCl_3 plasma. The SiO_2 mask is then removed by RIE with a CHF_3 plasma. The final step in the fabrication is the wet thermal oxidation of the $Al_{0.9}Ga_{0.1}As$ separation layer. Figure 4(b) shows several completed microlaser structures. Optical testing of the microlasers is currently underway.

a) b)

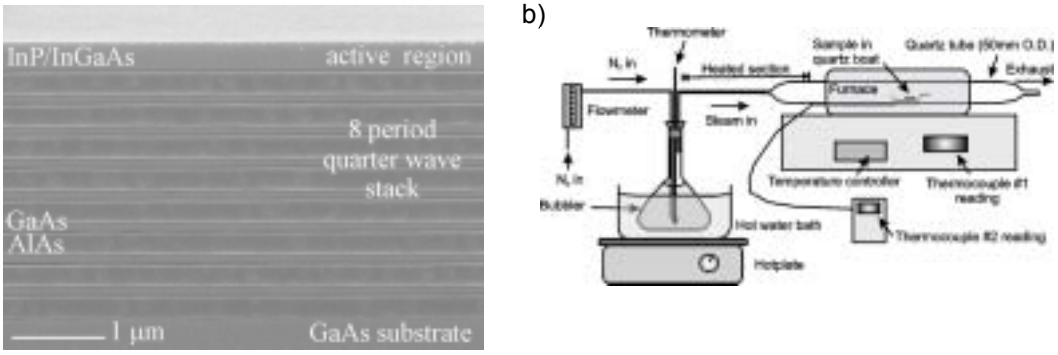

Figure 5. a) Cross-sectional scanning electron micrograph of the SBR material system. b) The oxidation apparatus.

Large Scale Oxidation of AlAs Layers for Broadband Saturable Bragg Reflectors

The conversion of AlGaAs alloys to Al_xO_y has received much attention for a wide variety of applications. Rarely, however, do such applications require large-scale lateral oxidation (i.e. 100s of microns). Oxidation of AlAs to Al_xO_y for use as a broadband saturable Bragg reflector (SBR) requires an Al_xO_y/GaAs mirror with lateral dimensions greater than 300 μm. For the SBR structure described below, the simulated bandwidth extends from 1200 nm to 1800 nm with greater than 99.5% reflectivity.

The layers within the SBR are grown using gas-source molecular beam epitaxy and are shown in Figure 5(a). The SBR structure contains an 8 period GaAs/AlAs quarter-wave stack grown on a GaAs substrate. The Al_xO_y layer is initially grown as AlAs that is later oxidized. The AlAs layer thickness corresponds to a quarter wavelength in Al_xO_y (n=1.66) plus a 10% shrinkage upon oxidation. The active region consists of an InP/InGaAs quantum well emitting near λ=1550 nm. The InP/InGaAs active region is not lattice-matched to the GaAs substrate and hence a defective interface exists between the active region and the Bragg reflector.

The AlAs is converted to Al_xO_y using a thermal oxidation process [apparatus shown in Figure 5(b)]. The structure was oxidized using a constant flow of N_2 bubbled through deionized water maintained at a constant temperature of 90ºC. The oxidation was performed at several different furnace temperatures. From 435ºC to 415ºC delamination of the active region occurs due to high interfacial stress upon oxidation. Sufficient lateral oxidation depths of over 300 μm are achieved, however, when the temperature is reduced to 400ºC (Figure 6). As an example of an application of the broadband SBR, the structure was utilized to initiate lasing in a Cr^{4+}:YAG laser. High-reflectivity, wide stop-band, and low loss are required for the Cr^{4+}:YAG laser cavity. With the oxidized SBR as an end mirror, self-starting with pulses as short as 35 fs have been achieved with Kerr lens mode-locking.

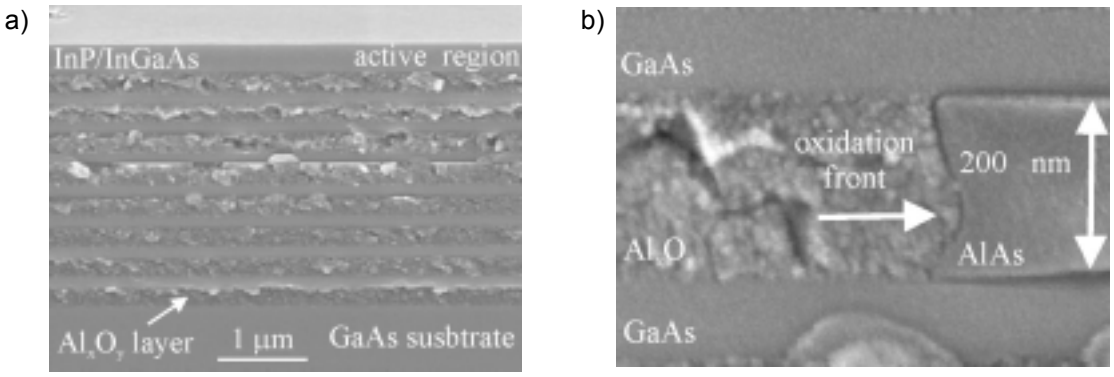

Figure 6. a) SEM cross-section of SBR structure oxidized at 400ºC. b) A magnified view of the oxidation front in one SBR period.

4. Guiding Light Through Sharp Bends Using Two Dimensional Photonic Crystals

Project Staff:
Solomon Assefa, Alexei A. Erchak, Daniel J. Ripin, Steven G. Johnson, Mark Mondol, Dr. Gale S. Petrich, Professor Erich P. Ippen, Professor John D. Joannopoulos, Professor Henry I Smith and Professor Leslie A. Kolodziejski

Sponsors:
National Science Foundation #DMR-9808941

The current effort to make integrated optical chips requires guiding light around sharp corners with a radius of curvature on the order of a wavelength. Light propagates in conventional waveguides as a result of total internal reflection at the interface between the high-refractive index guiding layer and its low-index surroundings. However, bends in the conventional index-contrast waveguides are susceptible to large optical losses depending on the radius of curvature of the bend. These optical losses, due to radiation, can be avoided by using a two-dimensional (2D) photonic crystal.

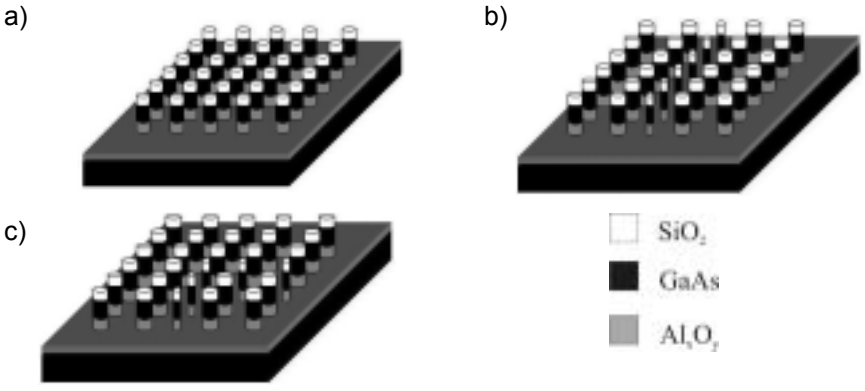

Figure 7. a) A photonic crystal. b) A linear waveguide consisting of cylinders with a smaller diameter within a photonic crystal. c) A 90º bend in the waveguide embedded in the photonic crystal.

The 2D photonic crystal consists of a periodic array of cylindrical rods of high dielectric material residing on a low dielectric material. Introducing a line defect, such as a row of cylinders with a different radius, into the 2D photonic crystal results in a linear waveguide. The radius of the cylinders in the line defect remains large enough to provide index guiding in the vertical dimension (normal to the plane of

periodicity). The periodic arrangement of dielectric rods surrounding the line defect creates a photonic band gap (PBG) i.e. a range of frequencies in which light cannot propagate. Thus, an optical signal with a frequency within the PBG has its energy confined in the line defect and evanescently decays into the photonic crystal. The localization of a mode inside the line defect can be utilized to guide light around sharp corners including a 90º bend with low optical loss. Figure 7 shows a photonic crystal (a), a linear waveguide consisting of cylinders with a smaller diameter within a photonic crystal (b) and a 90º bend within the photonic crystal (c).

The cylindrical rods of the photonic crystal consist of a high-index, 860 nm thick epitaxial layer of GaAs between a 300 nm thick SiO_2 cap layer and a 640 nm thick low-index Al_xO_y layer. An additional 860 nm thick Al_xO_y layer resides below the cylindrical rods in order to isolate the GaAs guiding layer from the GaAs substrate. The heterostructure is grown using gas source molecular beam epitaxy on a (100) GaAs substrate. The Al_xO_y is initially grown epitaxially as AlGaAs.

The fabrication process commences by sputtering a 300 nm thick SiO_2 layer on the sample. Next, the waveguide and photonic crystal are defined by using direct-write electron-beam lithography. Each sample is coated with polymethyl methacrylate (PMMA) electron-beam resist. Although each cylinder is defined by exposing a square pattern, the finite width of the beam rounds-off the corners of each square yielding a circular hole upon development. Simulations show that the largest band gap is obtained from a periodic arrangement of rods with a diameter of 300 nm. To observe a shift in the frequency range of the PBG, photonic crystals with cylinder diameters ranging from 270 nm to 330 nm are fabricated. Exposure-dose experiments are done to find the optimal parameters for the exposures. As shown in Figure 8, a dose of 375 μC/cm^2, current of 50 pA, and clock frequency of 0.09 MHz yield hole diameters close to the desired values. The input and output coupling waveguides and different sized arrays of holes are written by stitching 250 μm fields together.

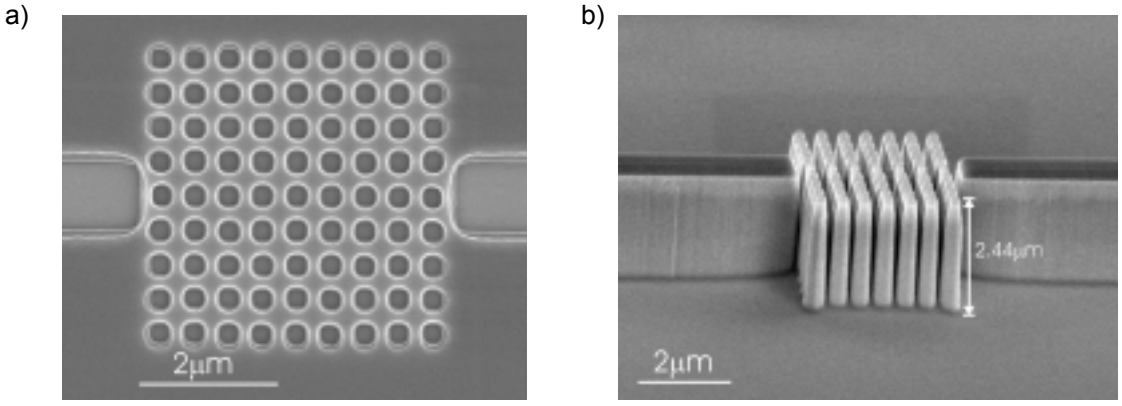

Figure 8. a) Top view SEM of e-beam written patterns of photonic crystal in PMMA. b) Side view SEM of a photonic crystal etched in GaAs using BCl_3 plasma

A 50 nm thick film of nickel is evaporated on the sample after the PMMA is developed, and a liftoff process is performed. The pattern is transferred to the SiO_2 by reactive-ion etching (RIE) in a CHF_3 plasma, after which a nickel etchant is used to remove the nickel mask. Using the patterned SiO_2 layer as a hard mask, the cylindrical rods are created by etching the GaAs and the AlGaAs to a total depth of 1.5 μm in a BCl_3 plasma. During the BCl_3 etch, the power and the DC bias are carefully monitored to control the etch rate and to avoid sputtering the SiO_2 mask, hence eliminating micromasking. Also, the etching is done at low pressure and low flow to minimize the formation and excessive deposition of polymers on the mask and the waveguide sidewalls. As more material is etched, the aspect ratio of the cylinders increases; lowering the BCl_3 flow minimizes microloading by increasing the number of radicals and ions available at the surface of the sample. This etching process leaves behind approximately 250 nm of the SiO_2 mask. Next, the AlGaAs is transformed into Al_xO_y using a wet thermal oxidation process. Finally, each substrate is lapped and the sample is cleaved in order to create a smooth input facet to promote the efficient coupling of a test signal with a wavelength of 1.55 μm.

The fabrication of the 2D photonic crystal waveguide structures is near its completion. Different configurations of input and output coupling waveguides are currently under investigation in an effort to minimize coupling loss due to reflections at the edge of the photonic crystal. One configuration under investigation is shown in Figure 9. The input waveguide is inserted into the photonic crystal and tapered to a width of 300 nm. The output waveguide is inverse-tapered and also starts inside the photonic crystal.

In the near future, transmission through the various structures will be measured. Of particular interest is the size of the photonic bandgap and the transmission through a line defect waveguide. Coupling losses at the input and output of the 2D photonic crystal waveguide will be investigated. Finally, the transmission through a sharp 90º bend will be measured and compared to theoretical simulations.

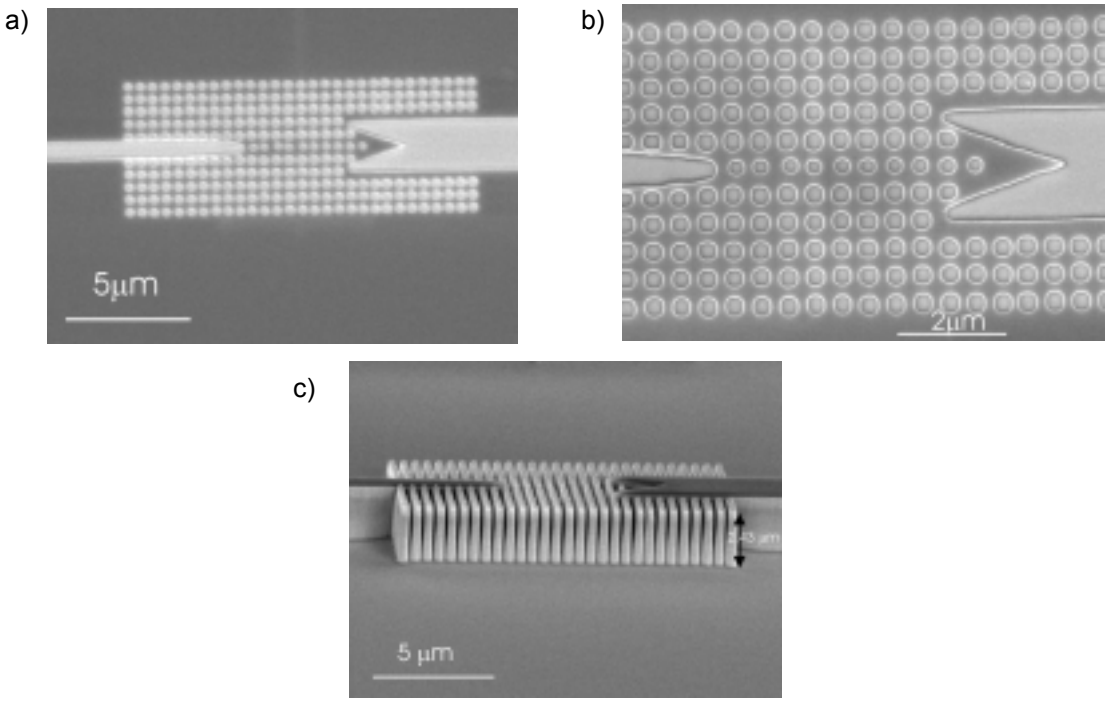

Figure 9. a) Plan view SEM micrograph of an electron-beam written linear-defect with tapered input and output coupling waveguides in PMMA. b) Magnified view of the line-defect waveguide with tapered input and output waveguides in PMMA. c) Side view SEM micrograph of same design after pattern transfer into GaAs using BCl_3 plasma.

5. GaAs Superprism Using Two Dimensional Photonic Crystals for Enhanced Beam Steering

Project Staff
Sheila Tandon, Alexei A. Erchak, Chiyan Luo, Marin Soljacic, Michael E. Walsh, Dr. Gale S. Petrich, Professor John D. Joannopoulos, Professor Henry I Smith and Professor Leslie A. Kolodziejski

Sponsor
Rockwell Science Center: #B1F431652

A superprism is an optical device similar to a conventional prism only with two enhanced properties: (1) super-dispersion and (2) ultra-refraction. Just as a conventional prism separates light into multiple wavelengths, a superprism separates these wavelengths over wider angles--termed "super-dispersion." A superprism can also be used to magnify the angle of propagation of a single wavelength of light to steer the beam over wide angles--termed "ultra-refraction." Photonic crystals form the essence of the superprism effect. The highly anisotropic nature of photonic crystals makes propagation of light through

the superprism very sensitive to changes in direction and frequency. Being able to realize these superprism effects would be very useful for a number of applications ranging from enhanced devices for wavelength division multiplexed (WDM) systems to a new class of ultra-refractive optical elements for beam manipulation. An additional advantage of the superprism is its potential to reduce the size of many conventional optical systems.

The device consists of a two dimensional photonic crystal with a square lattice of cylindrical air holes in a GaAs layer. The top view of the device design shows how the GaAs region is shaped as a parallelogram with the photonic crystal occupying a square region within the parallelogram (Figure 10). The input and output of the device are the edges of the parallelogram shape. The initial design has focused on realizing ultra-refraction such that an input angular sweep of approximately +/- 2 degrees is amplified to about +/- 30 degrees at the output for light with a wavelength of 3.2 microns. A thick aluminum oxide (Al_xO_y) layer is used to minimize radiation loss into the GaAs substrate. The depth of the holes will be as deep as possible to facilitate coupling from an input fiber.

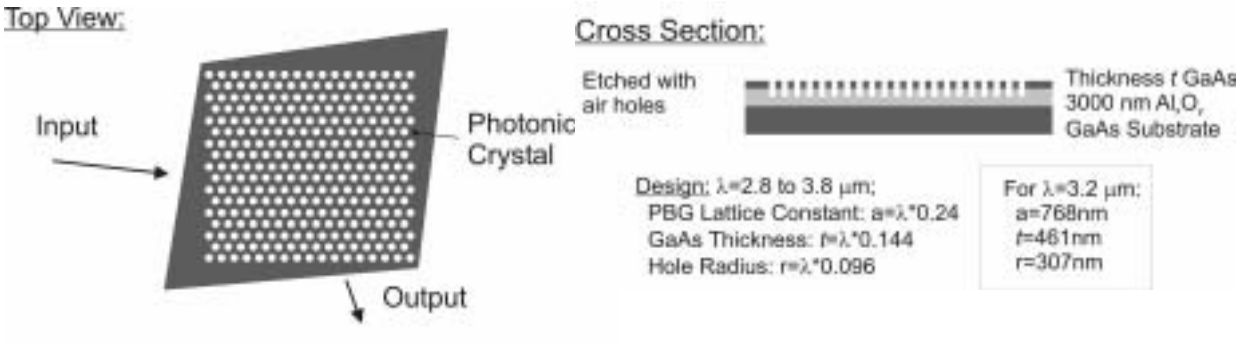

Figure 10. Superprism device design.

The feature sizes of the photonic crystal can be scaled depending on the wavelength of operation. A desired wavelength range of 2.8 to 3.8 microns implies a lattice constant of 672 to 912 nm, and a hole radius varying between 269 and 365 nm, respectively. The total thickness of the device (excluding the substrate) is about 3.5 microns (460 nm GaAs, 3 μm Al_xO_y) while the top surface will have an area of about 2x2 cm.

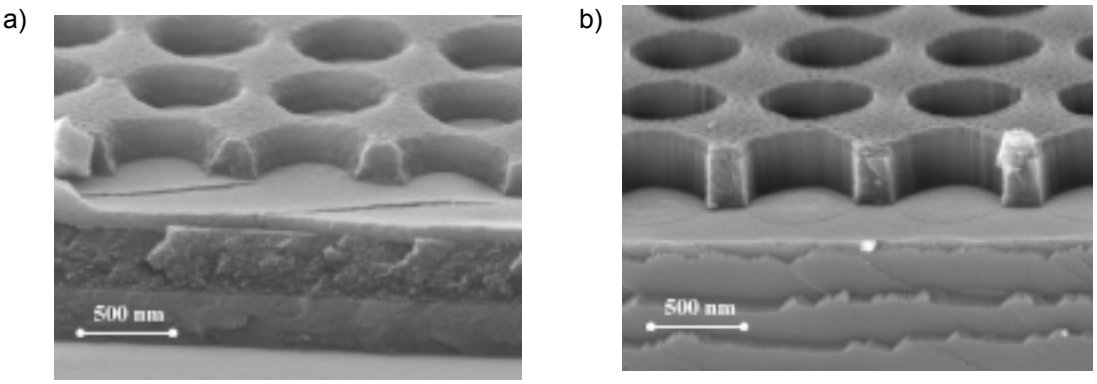

Figure 11. Results of interference lithography exposure using the Lloyd's mirror. a) The pattern in resist with a 90nm thick SiO_2 interlayer, a 300nm thick antireflective coating, and a 250 nm thick SiO_2 hard mask layer on a GaAs substrate. b) The pattern in the SiO_2 hard mask layer after reactive ion etching.

Interference lithography (IL) is used to pattern the photonic crystal holes due to the need to create a periodic pattern covering a large area with feature sizes less than one micron. A trilayer resist stack of resist, SiO_2, and an anti-reflection coating (ARC) is used to minimize reflections off the substrate during

exposure from a HeCd laser source (λ=325 nm). Figure 11(a) shows the results of an IL exposure using the Lloyd's mirror with the trilayer resist stack. The period is about 750 nm. Figure 11(b) shows the results after the pattern is transferred to a 250 nm thick SiO_2 hard mask layer using reactive ion etching.

The heterostructure will be grown using gas source molecular beam epitaxy on a (100) GaAs substrate. The large parallelogram and square shapes will be made using contact photolithography. All patterns will be transferred to the GaAs/AlGaAs epilayers using reactive ion etching. A wet oxidation step will be used to oxidize the AlGaAs layer creating the low index Al_xO_y layer. Careful alignment steps must be used to ensure that lines of photonic crystal holes are aligned to the edges of the large square area.

6. A GaAs-based Optical Nanoelectromechanical Device

Project Staff
Reginald E. Bryant, Alexei A. Erchak, Solomon Assefa, Daniel J. Ripin, Peter Rakich, Michelle L. Povinelli, Dr. Gale S. Petrich, Professor Erich P. Ippen, Professor John D. Joannopoulos, and Professor Leslie A. Kolodziejski

Sponsors:
National Science Foundation #DMR-9808941

Optical systems are being developed to reach the functionality and large-scale integration of electronic systems. Strides are being made to develop an on-chip optical system by designing and fabricating an optical nanoelectromechanical, ONEM, device structure based in a gallium arsenide material system. The GaAs, a III-V compound semiconductor, was chosen due to its high-refractive index contrast when combined with oxidized AlAs. GaAs was specifically chosen over other III-V materials due to its comparable mechanical integrity to silicon-based electromechanical devices. The ONEM project will addresses several fabrication issues: nanometer-sized feature fabrication, optical wave guiding and mode-matching, and electronic and mechanical interactions in a gallium arsenide material system.

Developing an optical nanoelectromechanical switch presents a dynamic problem with design tradeoffs existing in both optical operation and electromechanical operation. Three-dimensional energy modeling simulations were carried out to determine the relationship between optical transmission and the deflection of the cantilever. Frequency-domain and time-domain simulations were used to simulate the optical performance of the various switch designs. Two-dimensional finite difference modeling simulations were carried out to determine the electromechanical operation of a nanometer-sized GaAs cantilever. The variational method and the Rayleigh-Ritz method were used to simulate the optical switch's electromechanical operation. The results of optical simulations and electromechanical simulations lead to an optimal device structure that is currently being fabricated.

The completion and testing of the optical switch should give insight on the capabilities of optical nanoelectromechanical devices fabricated in a GaAs material system. Resolving the issues facing nanometer-sized patterns and pattern transfer makes it possible to scale down current microelectromechanical (MEM) structures into the nanometer regime. Characterizing the electromechanical properties of GaAs would lead to the development of more complex ONEM structures. Resolving the issues facing optical confinement in a high contrast medium of gallium arsenide and aluminum oxide would make it possible to transfer the ONEM structure to other III-V material systems. Immediate goals are focused on increasing the on/off contrast of the switch by incorporating additional coupling waveguide elements and photonic crystals into the design with the long-range goal of creating a wavelength filter by the incorporation of photonic crystals.

Publications

Journal Articles, Published

Erchak, A. A., D. J. Ripin, S. Fan, P. Rakich, G. S. Petrich, L. A. Kolodziejski, E. P. Ippen, and J. D. Joannopoulos, "Enhanced Coupling to Vertical Radiation Using a Two-Dimensional Photonic Crystal in a Semiconductor Light-Emitting Diode." Appl. Phys. Lett., 78 (5), 563-565 (2001).

Gopinath, J. T., E. R. Thoen, E. M. Knootz, M. E. Grein, L. A. Kolodziejski, E. P. Ippen, "Recover Dynamics in Proton-bombarded Semiconductor Saturable Absorber Mirrors." Appl. Phys. Lett. 78 (22), 3409-3411 (2001).

Meeting Papers, Published

Erchak, A. A., D. J. Ripin, S. Fan, P. Rakich, G. S. Petrich, L. A. Kolodziejski, E. P. Ippen, and J. D. Joannopoulos, "Enhanced Emission from a Light-Emitting Diode Modified by a Photonic Crystal." Mat. Res. Soc. Symp. Proc. Pittsburgh, PA, USA, 637 (2001).